analysis of Sakata & Cooper. The agreement factor A_B [see (5)] in the conventional refinement reflects the degree of matching between the observed and calculated integrated intensities, whereas the agreement factor A_P [see (8)] for the Rietveld refinement reflects not only the degree of matching between integrated intensities but also that between the shape functions describing the profile of the individual reflections. The structural parameters are determined by the integrated intensities and the profile parameters by the shape functions: it is not surprising that the e.s.d.'s from the Rietveld refinement are different from those from the conventional refinement.

References

BACON, G. E. (1976). *Neutron Diffraction*, 3rd ed. Oxford Univ. Press.

BUSING, W. R., MARTIN, K. O., LEVY, H. A., ELLISON, R., HAMILTON, W. C., IBERS, J. A., JOHNSON, C. K. & THIESSEN, W. E. (1971). *ORXFLS* 3. Oak Ridge National Laboratory, Tennessee.

COOPER, M. J. & SAKATA, M. (1979). *Z. Kristallogr.* **149**, 337–338.

DOLLING, G., COWLEY, R. A. & WOODS, A. D. B. (1965). *Can. J. Phys.* **43**, 1397–1413.

GRONVOLD, F. (1955). *J. Inorg. Nucl. Chem.* **1**, 357–370.

HEWAT, A. W. (1973). Report RRL/73/187. AERE Harwell, Oxfordshire, England.

MALMROS, G. & THOMAS, J. O. (1977). *J. Appl. Cryst.* **10**, 7–11.

RIETVELD, H. M. (1967). *Acta Cryst.* **22**, 151–152.

RIETVELD, H. M. (1969). *J. Appl. Cryst.* **2**, 65–71.

ROUSE, K. D., WILLIS, B. T. M. & PRYOR, A. W. (1968). *Acta Cryst.* B**24**, 117–122.

SAKATA, M. & COOPER, M. J. (1979). *J. Appl. Cryst.* **12**, 554–563.

YOUNG, R. A., MACKIE, P. E. & VON DREELE, R. B. (1977). *J. Appl. Cryst.* **10**, 262–269.

Acta Cryst. (1980). A**36**, 270–276

The Diffraction Aspect and a Structural Model of Mullite, $Al(Al_{1+2x}Si_{1-2x})O_{5-x}$

BY M. TOKONAMI, Y. NAKAJIMA* AND N. MORIMOTO†

The Institute of Scientific and Industrial Research, Osaka University, Yamadakami, Suita, Osaka 565, *Japan*

(*Received* 16 *July* 1979; *accepted* 16 *October* 1979)

Abstract

Diffraction patterns of various specimens of mullite were recorded using a high-power X-ray generator. The patterns consist of main reflections based on the primitive orthorhombic lattice with $a = 7{\cdot}6$, $b = 7{\cdot}7$ and $c = 2{\cdot}9$ Å, and two types of subsidiary reflections. Although the patterns show no periodicity in reciprocal space, a periodic unitary intensity distribution is deduced using information from the average structure. The distribution of the sites of the removed oxygen atoms in the sillimanite-like ideal structure is obtained from the qualitative values of the unitary intensity. In order to compare the calculated value to the observed continuous intensity distribution in reciprocal space, a structural model was constructed. It contains four sorts of equivalent domains; each domain consists of about 40 000 atoms. These atoms are situated at definite positions in real space, and no partly occupied sites are specified in these models.

Introduction

Mullite, $Al(Al_{1+2x}Si_{1-2x})O_{5-x}$, is a typical non-stoichiometric compound, which ranges in composition from $3Al_2O_3.2SiO_2$ to $2Al_2O_3.SiO_2$. Although its X-ray diffraction patterns are very similar to those of sillimanite, mullite commonly shows diffuse scattering, as pointed out by Taylor (1928), and sometimes shows superlattice reflections as described by Agrell & Smith (1960).

Sadanaga, Tokonami & Takéuchi (1962) determined the average structure of mullite and clarified the structural relationship between mullite and sillimanite. Durovic (1962) independently analyzed the average structure. The results obtained by Sadanaga, Tokonami & Takéuchi (1962) were confirmed by Burnham (1964). It should be noted that Warren (1933) proposed the exact scheme for the mullite structure prior to the above authors.

* Present address: Department of Geological Sciences, Virginia Polytechnic Institute and State University, Blacksburg, VA 24061, USA.

† Present address: Geological & Mineralogical Institute, Faculty of Science, Kyoto University, Sakyo, Kyoto 606, Japan.

0567-7394/80/020270-07$01.00

In this paper, the intensity distribution of subsidiary reflections has been analyzed, and a superstructure model for mullite solid solution has been described.

Description of subsidiary reflections of mullite

Crystals synthesized by the electrical fusion method were studied by the precession method using a high-power X-ray generator (Mo $K\alpha$, 60 kV 500 mA). Typical precession photographs are shown in Fig. 1. The intensity distribution of subsidiary reflections coincides well with that described by Agrell & Smith (1960).

The subsidiary reflections are divided into two groups: the reflections of the first group consist of sharp and/or diffuse spots, of which intensity maxima occur at $l = L + 1/2$, $h = H \pm 2/7$ and $k = K$, where H, K and L are integers. Those of the second group consist of broad diffuse streaks, of which maxima are at $l = L \pm 2/9$ and extend along the lines of either $h + k = K \pm 4/7$ or $h - k = K \pm 4/7$. The intensity varies along the streaks and becomes strong when k approaches an integer. It almost vanishes when h is an integer. Although the peak intensity of the second group is far weaker than that of the first, the integrated intensity in reciprocal space is almost of the same magnitude.

Relation between the intensity distribution of subsidiary reflections and the superstructure

The origin of the superstructure of mullite results from the statistical removal of oxygen atoms from O(3) sites which causes a corresponding positional shift of the related tetrahedrally coordinated metal atoms in the sillimanite-like ideal structure. Since the shift of the neighbors has been described by the analysis of the average structure, a superstructure model can be constructed by specifying the vacant positions of the O(3) sites. The known data on the average structure, which is necessary for the present analysis is summarized in Table 1. Since the base center $(\frac{1}{2},\frac{1}{2},0)$ is equivalent to the origin in the space group *Pbam*, the O(3) sites make a lattice complex which is a *C*-centered lattice with the same cell dimensions as the primitive lattice of the average structure. This lattice complex is hereafter referred to as the O(3) sublattice.

If the distribution of vacancies has a three-dimensional long-range periodicity, the entire structure can be described by a table of the position of each vacancy in the superlattice. However, because no long-range periodicity exists in the superstructure of mullite, it is not possible to complete such a table of finite size. In this paper, a method by which the arrangement of vacancies in the superstructure can be specified has been derived based on the O(3) sublattice.

Table 1. *Crystal data and parameters of the relevant atoms in the ideal and the average structure of mullite*, $Al(Al_{1+2x}Si_{1-2x})O_{5-x}$

Cell edges $a = 7{\cdot}6$, $b = 7{\cdot}7$, $c = 2{\cdot}9$ Å
Space group *Pbam*

Atom	Occupancy	Coordinates		
		x	y	z
$M(1)$	$1-x$	0·149	0·159	0
$M(2)$	x	0·264	0·294	0
O(3)	$1-3x$	0·000	0·000	0
O(4)	$2x$	0·447	0·447	0

Isotropic temperature factor $B = 1{\cdot}2$ Å^2

Composition

$x = 0$	for ideal structure
$x = 0{\cdot}125$–$0{\cdot}2$	for average structure

The coordinates are obtained by the following equations: $x = -x' + \frac{1}{4}$, $y = y'$, $z = z' - \frac{1}{4}$, where primed coordinates are those given by Sadanaga, Tokonami & Takéuchi (1962).

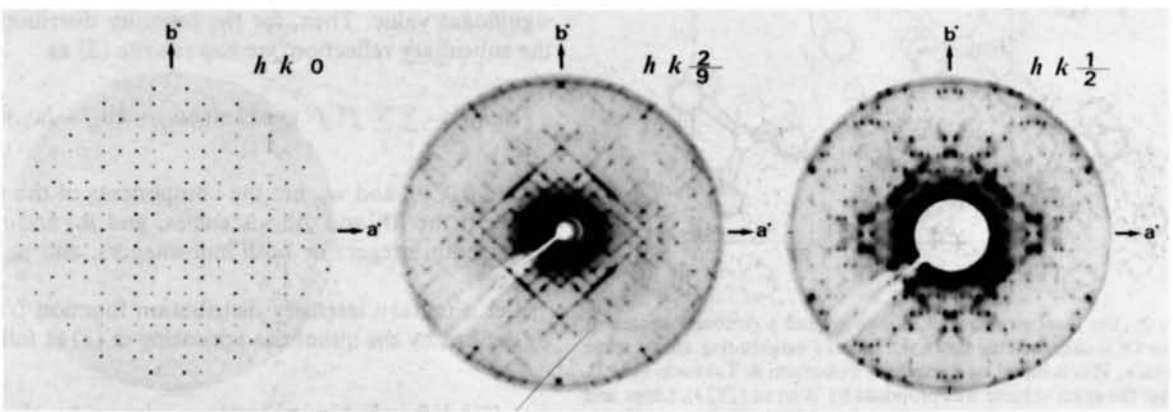

Fig. 1. Precession photographs of mullite.

Let the crystal structure factor of the ideal structure of mullite be $F_{\text{ideal}}(h,k,l)$. If an oxygen atom at the corner of a unit cell in the O(3) sublattice at $N_1\mathbf{a} + N_2\mathbf{b} + N_3\mathbf{c}$ is removed, two adjacent tetrahedrally coordinated metal atoms at $M(1)$ sites move to the neighboring $M(2)$ sites, and two adjacent oxygen atoms at O(3) sites move to the nearer O(4) sites as shown in Fig. 2. The expression for the structure factor, $F_{\text{vac}}(h,k,l)$, which results from the removal and shifts is

$$\begin{aligned}F_{\text{vac}}(h,k,l) = \exp[2\pi i(hN_1 + kN_2 + lN_3)] \\ \times \{f_O[-1 - 2\cos\pi(h+k) \\ + 2\cos 2\pi(0{\cdot}447h + 0{\cdot}447k)] \\ + f_M[-2\cos 2\pi(0{\cdot}149h + 0{\cdot}159k) \\ + 2\cos 2\pi(0{\cdot}264h + 0{\cdot}294k)]\},\end{aligned}$$

where f_O and f_M are the atomic structure factors of oxygen and the tetrahedrally coordinated metal atoms respectively. Likewise, the removal of an oxygen atom at the base center of a unit cell results in an expression for the structure factor,

$$\begin{aligned}F_{\text{vac}}(h,k,l) = \exp[2\pi i(hN_1 + kN_2 + lN_3 + h/2 + k/2)] \\ \times \{f_O[-1 - 2\cos\pi(h-k) \\ + 2\cos 2\pi(0{\cdot}447h - 0{\cdot}447k)] \\ + f_M[-2\cos 2\pi(0{\cdot}149h - 0{\cdot}159k) \\ + 2\cos 2\pi(0{\cdot}264h - 0{\cdot}294k)]\}.\end{aligned}$$

The structure factor $F(h,k,l)$ of real mullite, in which the jth vacancy occupies the O(3) site at $(N_1^j + n^j)\mathbf{a} + (N_2^j + n^j)\mathbf{b} + N_3^j\mathbf{c}$, where n^j is equal to zero or one half, is therefore given by

$$\begin{aligned}F(h,k,l) = F_{\text{ideal}}(h,k,l) + \sum_j f^j \exp\{2\pi i[h(N_1^j + n^j) \\ + k(N_2^j + n^j) + lN_3^j]\},\end{aligned}$$

$$\begin{aligned}f^j = f_O[-1 - 2\cos\pi(h \pm k) + 2\cos 2\pi(0{\cdot}447h \\ \pm 0{\cdot}447k)] + f_M[-2\cos 2\pi(0{\cdot}149h \pm 0{\cdot}159k) \\ + 2\cos 2\pi(0{\cdot}264h \pm 0{\cdot}294k)], \qquad (1)\end{aligned}$$

where the double sign should be regarded as positive when n^j is zero and negative when n^j is one half. The values of f^j vary rather slowly in reciprocal space. Specifically, the variation of the value of l has little effect on f^j. However, the values of f^j oscillate between about +24 and −28 according to changes of h and k values.

The intensity distribution $I(h,k,l)$ is represented by

$$\begin{aligned}I(h,k,l) = F_{\text{ideal}}(h,k,l)\,F^*_{\text{ideal}}(h,k,l) \\ + F_{\text{ideal}}(h,k,l)\sum_j f^j \exp\{-2\pi i[h(N_1^j + n^j) \\ + k(N_2^j + n^j) + lN_3^j]\} \\ + \sum_j f^j \exp\{2\pi i[h(N_1^j + n^j) \\ + k(N_2^j + n^j) + lN_3^j]\}\,F^*_{\text{ideal}}(h,k,l) \\ + \sum_i\sum_j f^i f^j \exp\{2\pi i[h(N_1^i - N_1^j + n^i - n^j) \\ + k(N_2^i - N_2^j + n^i - n^j) + l(N_3^i - N_3^j)]\}. \qquad (2)\end{aligned}$$

Because of the periodicity of ideal structure, $F_{\text{ideal}}(h,k,l)$ is zero except at the exact reciprocal-lattice points. If at least one of h, k and l is not an integer, the first three terms in (2) are zero, and only the fourth term has a significant value. Then, for the intensity distribution of the subsidiary reflection, we can rewrite (2) as

$$I(h,k,l) = \sum_i\sum_j f^i f^j \exp[2\pi i(hu_{ij} + kv_{ij} + lw_{ij})], \quad (3)$$

where u_{ij}, v_{ij} and w_{ij} are the components of the vector between the ith and jth vacancies, and u_{ij} and v_{ij} are either both integers or both half integers, and w_{ij} is an integer.

Let a unitary intensity distribution function $U(h,k,l)$ be defined by the quantities appearing in (3) as follows:

$$U(h,k,l) = \sum_i\sum_j \exp[2\pi i(hu_{ij} + kv_{ij} + lw_{ij})]. \qquad (4)$$

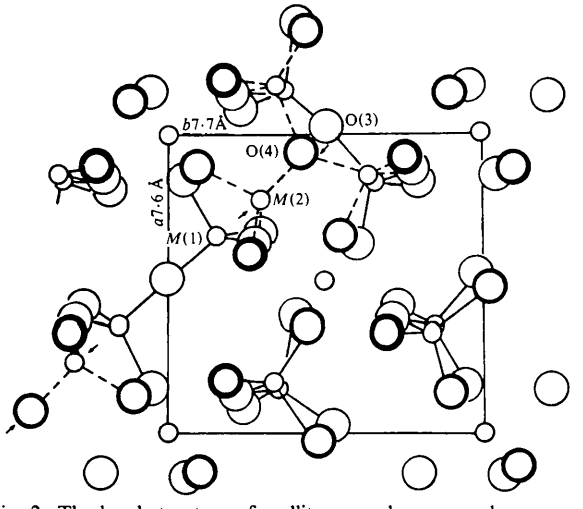

Fig. 2. The local structure of mullite around a removed oxygen at an O(3) site, showing how migration of neighboring atoms takes place. This is based on Sadanaga, Tokonami & Takéuchi (1962), but the exact scheme was proposed by Warren (1933). Large and small circles represent oxygen and metal atoms, respectively. A unit cell is drawn after Sadanaga, Tokonami & Takéuchi (1962).

Because all of u_{ij}, v_{ij} and w_{ij} are integers or half integers, $U(h,k,l)$ is a three-dimensional periodic function with period not greater than two. Therefore, if $U(h,k,l)$ is evaluated in appropriate regions, the behavior of $U(h,k,l)$ throughout reciprocal space is simultaneously determined. In fact, there are some regions in which the ratio of two possible values of f^j is nearly equal to unity. In such a region, an approximate value of $U(h,k,l)$ may be calculated by

$$U(h,k,l) = I(h,k,l)/\bar{f}^2, \tag{5}$$

where $\bar{f}$ represents the average value of f^j. Thus, the approximate value of the unitary intensity distribution can easily be obtained from the observed intensity distribution.

The distribution of the inter-vacancy vectors, $P(u,v,w)$ is represented by the Fourier transform of $U(h,k,l)$ as follows,

$$P(u,v,w) = \int_{hkl} U(h,k,l) \exp[-2\pi i(hu + kv + lw)] \, dh \, dk \, dl. \tag{6}$$

Owing to the orthogonality of the exponential function, $P(u,v,w)$ is proportional to the number of coincidences between (u,v,w) and (u_{ij},v_{ij},w_{ij}) appearing in (4). Although $P(u,v,w)$ and $U(h,k,l)$ are defined as a Patterson function and an intensity distribution function, and their physical meanings are the same as those commonly used, their nature is slightly different from the case of conventional crystal-structure analysis. In the conventional case, u, v and w are continuous variables and the Patterson map has periodicity, while, in this case, $P(u,v,w)$ is not trivial only when u, v and w are all integers or half integers.

Characteristic features of the distribution of inter-vacancy vectors

To know the characteristic features of $P(u,v,w)$, the following two properties of $U(h,k,l)$, which are inherited from the observed intensity distribution, are utilized:

(1) $U(h,k,l)$ takes a trivial value except at (H,K,L), near $(H \pm 2/7, K, L + 1/2)$ and near $(r, K \pm r \pm 4/7, L \pm 2/9)$, where r is a real number and H, K and L are integers.

(2) The integrated value of $U(h,k,l)$ over the whole h and k and around $l = \pm 2/9$ is almost the same as that around $l = \frac{1}{2}$.

Judging from the fact that $U(h,k,0)$ takes a significant value only when both h and k are integers, we can conclude that the two-dimensional projection along the c axis has no superstructure and that each row of the O(3) sublattice parallel to the c axis is equivalent. Therefore, the probability of a vacancy in each row is equal to the x value appearing in the chemical formula.

In order to find the one-dimensional arrangement of the vacancy in the rows parallel to the c axis,

$$P(0,0,w) = \int_l \left[\int_{hk} U(h,k,l) \, dh \, dk \right] \exp(2\pi i l w) \, dl \tag{7}$$

will be considered. The integrated values of $U(h,k,l)$ around $l = 1/2$ and $l = 2/9$ are large, so that $P(0,0,w)$ cannot be large when w is a small odd number, *i.e.* $P(0,0,1)$ and $P(0,0,3)$ may be assumed to be zero. Moreover, $P(0,0,2)$ is small because the integrations of U around $l = 1/2$ and $l = 2/9$ contribute with opposite sign and almost the same magnitudes in (7). Since the integrated value of U around $l = 2/9$ is large, $P(0,0,w)$ is large when w approaches 9/2. According to these considerations, most of the inter-vacancy periods along the c axis are $4c$, and somewhat longer intervals are also expected. Many models of the one-dimensional point sets satisfying the above conditions have been constructed, and the Fourier transformation of their vector sets have been calculated and compared with $\int U(h,k,l) \, dh \, dk$. A pair of simple models with period of $27c$ are found to give the best correspondence with the observed data (Fig. 3). In these models, four vacancies are equally separated by $4c$ intervals to produce an area of high vacancy density, and two other vacancies in a unit translation sit between these dense parts.

The two-dimensional distribution of vacancies on $(\bar{1}10)$, which is one of the densest net planes of the O(3) sublattice, will now be discussed. The information about the distribution can be obtained from the two-dimensional Patterson map $P(u,u,w)$. Substituting v by u in (6), we obtain

$$P(u,u,w) = \int_{rkl} U(r, k-r, l) \exp[-2\pi i(ku + lw)] \times dr \, dk \, dl. \tag{8}$$

This can be written as in the following equations:

$$P(u,u,w) = \int_{kl} p(k,l) \exp\{-2\pi i(ku + lw)\} \, dk \, dl$$

$$p(k,l) = \int_r U(r, k-r, l) \, dr. \tag{9}$$

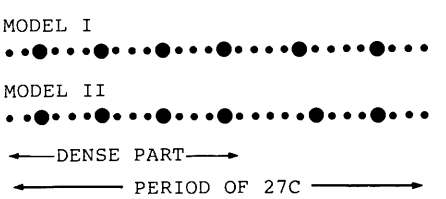

Fig. 3. Distribution of vacancies in a [001] row line of the O(3) sublattice. Two simple models with periods of $27c$ are shown. Groups of a few vacancies make dense parts in the structure. Large and small circles represent vacant and occupied sites, respectively.

Since the diffraction patterns show streaks along (r, 4/7 − r, −2/9), $p(k,l)$ is large when $k = 4/7$ and $l = -2/9$. Consequently, $P(u,u,w)$, which is the two-dimensional Fourier transform of p, has significant values when $4u/7 - 2w/9$ is nearly equal to an integer. Putting $u = 1/2$, this condition is fairly well satisfied when $w = 2$ and $w = -4$. Putting $u = 7/2$, it is exactly satisfied when $w = 9$. This results in one and only one arrangement of the area of high vacancy density with $4c$ intervals, as illustrated in Fig. 4. In this arrangement, the vacancies concentrate along the [7,7,18] zone axis. The rest of the vacancies are distributed in relatively narrow bands between the high vacancy density areas.

To explain the diffuse streaks perpendicular to this plane, it is necessary to build up a three-dimensional superlattice with more than one stacking vector (Dornberger-Schiff, 1956). However, the main reflections and the subsidiary reflections of the first group have no streaks around them. This fact indicates that the averaged structure with the doubled periods of c axis has a regular three-dimensional lattice with a definite stacking vector. Because these reflections display no irregularity along the b axis, the stacking vector in this averaged structure is defined to be [010]. This means that the stacking vectors in the true superstructure are represented by [0,1,2n], because two vectors which differ from each other by [002] coincide in this averaged structure.

The intensity distribution of the subsidiary reflections of the second group depends on the stacking sequence of the densest planes. The average direction of the stacking vectors will be represented by [01q]. As the vacancies concentrate along [7,7,18] and at the same time along [01q], they must concentrate near (18 − 7q, 7q, −7) planes. For example, if ($\bar{1}$10) planes are stacked by a statistical succession of five [010] stacking vectors and nine [012] stacking vectors, the average direction of them becomes [0,1,9/7], and there appears a diffuse maxima in the diffraction pattern corresponding to planes parallel to (99$\bar{7}$).

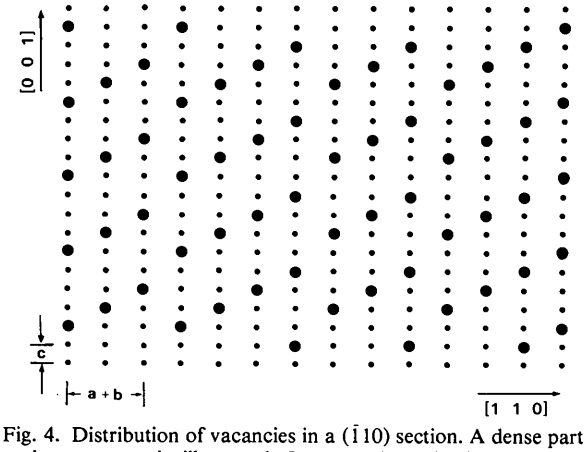

Fig. 4. Distribution of vacancies in a ($\bar{1}$10) section. A dense part in the structure is illustrated. Large and small circles represent vacant and occupied sites, respectively.

These considerations result in the superstructure models of mullite. The choice of the most preferable model must be based on a comparison of the observed and calculated intensity distribution.

The structure thus obtained is based on the diffuse streaks along (r, 4/7 − r, −2/9). The other three types of diffuse streaks along (r, 4/7 − r, 2/9), (r, 4/7 + r, −2/9) and (r, 4/7 + r, 2/9) are symmetrically related to (r, 4/7 − r, −2/9). They are related by a mirror across (001), a mirror across (010) and a twofold rotation axis about [100], respectively. The entire intensity distribution is explained by a domain structure of these four equivalent superstructures.

The calculation of the intensity distribution

The vacancy distribution in the preceding section has a slightly greater number of vacancies than that expected from the chemical composition. The proportion of vacancies to O(3) sites is 2/9 in the above model, while it is generally less than 2/10 in most specimens. Some part of this discrepancy results from the simplifying assumption used in the mathematical treatment that two oxygens at adjacent O(3) sites can be removed simultaneously. However, $P(\pm\frac{1}{2},\frac{1}{2},0)$ is always equal to zero in a real crystal, because at least one of the oxygens at the adjoining O(3) sites must be coordinated to the metal atom between them. Therefore, if two vacancies were to occupy an adjoining pair in the O(3) sublattice of the model, the intermediate metal atom could not be appropriately coordinated to the required four oxygen atoms, and the structure would no longer be stable. This consideration decreases the number of vacancies in the structure to an appropriate value which corresponds to the compositional restrictions.

In order to confirm the proposed superstructure model, the intensity distribution was calculated and compared with the observed distribution. For calculation purposes, each model is considered to have a convenient size and consist of four domains in twin relation. The domains are assumed to have a parallelepiped shape with the dimensions $7(\mathbf{a} + \mathbf{b}) \times 14\mathbf{b} \times 27\mathbf{c}$. For a domain consisting of about 40 000 atoms, the evaluation of the structure factors with the usual formula requires a great deal of calculation. However, based on (1), it is easily carried out by summing less than 1000 terms of the geometrical phase factors multiplied by either of the two kinds of scattering factors of f^j. The weighted mean value of the scattering factor for Al^{3+} and Si^{4+} given by Cromer & Mann (1968) and that for O^{2-} given by Tokonami (1965) have been used in the calculation of f^j. The sum of the intensities of the four incoherent domains has been calculated for each of about 200 000 sampling points in reciprocal space,

for which $(h,k,l) = (H/14,K/14,L/27)$, where H and K are integers smaller than 85 and L is an integer smaller than 28. The calculated intensity distributions have been compared with the observed intensities. If the calculated values are significant at some point in reciprocal space where significant intensity is not observed, then the model is discarded.

Among the models which give significant intensities at appropriate positions, there are a few which show good agreement with the observed intensity distribution. One of them is built by the following process. The possible vacancy sites are concentrated near one of the six regularly separated planes parallel to $(99\bar{7})$ in a domain. The change of the z coordinate against the x and y coordinates is illustrated in Fig. 5. The z coordinates of the other possible sites are obtained by adding one of 4, 8, 12, 17 and 22 to the z values in the figure. If the value exceeds 27, then the new value is given by subtracting 27. Thus, 1176 sites are generated. After the elimination of vacancies which are adjacent at the same value of z, the number of vacancies becomes 984 and the chemical composition in a domain is $(Al_2O_3)_{6276}(SiO_2)_{3324}$. The calculated intensity distributions on $(h,k,2/9)$ and $(h,k,1/2)$ are shown in Fig. 6, which correspond very closely to the diffraction patterns shown in Fig. 1. Other models which are able to explain minor intensity differences observed in the diffraction patterns of different mullite specimens can be obtained by making some minor changes to this model. Even after these changes, the basic arrangement in the area of high valency density of the $4c$ intervals is untouched. The peak values of diffuse maxima in the calculated intensity distribution are rather sensitive to these minor changes. However, so far as the integrated values over appropriate volumes in reciprocal space are concerned, the intensity distributions are very similar for most of the models.

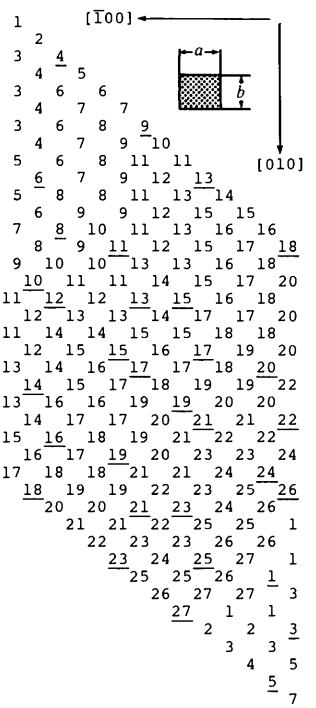

Fig. 5. Change of the z coordinates of vacancies at the O(3) sublattice. Only vacancies near $(99\bar{7})$ are shown. Underlined sites are the potential vacancy sites which must be occupied due to the restrictions imposed by considering the effect of adjacent vacancies on the structure.

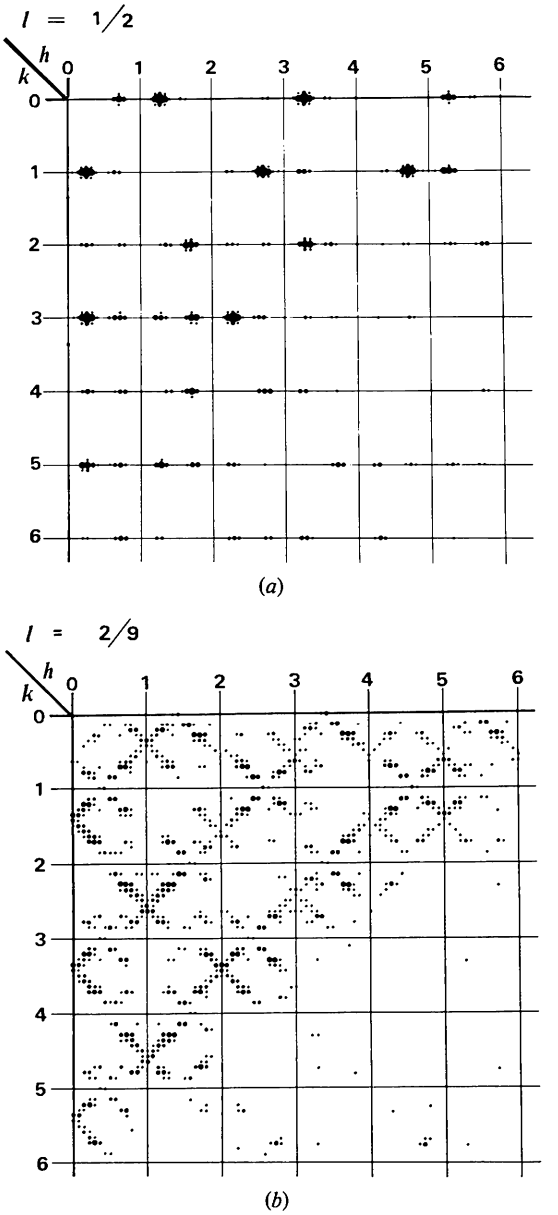

Fig. 6. Calculated intensity distribution in reciprocal space. (*a*) The section at $l = 1/2$. (*b*) The section at $l = 2/9$. The area of each circle is approximately proportional to the intensity. The intensities weaker than that scattered by two electrons per vacancy are omitted.

Discussion

The above model consists of domains of lower symmetry than that of the ordered structure. This domain structure suggests that the superstructure is not a relic of growth but is rather the product of phase changes. When the mullite crystals grow at high temperature, the vacancies are in a random distribution. As the temperature decreases, the vacancies tend to order as follows. Three or four vacancies make linear clusters extending along [112]. The linear clusters gather together to make a planar cluster parallel to $(99\bar{7})$. Several planar clusters are distributed with $4c$ intervals along the c axis to make a three-dimensional dense volume of vacancies, and several dense volumes are connected to make an individual domain. Several domains in twin relation are distributed in the whole mullite crystal. Thus, the number and the size of the domains depend on the cooling history as well as the chemical composition of the crystal. *D*- and *S*-mullite, named by Agrell & Smith (1960), may correspond to ill and well ordered specimens, respectively. One of the most ordered specimens is described by Nakajima, Morimoto & Watanabe (1975).

Guse & Saalfeld (1976) have insisted that the subsidiary reflections of the first group reflect the superstructure, and that the other subsidiary reflections arise from different physical phenomena such as lattice strain. However, the information obtained from the main reflections and the first group reflections is related only to the average structure with the doubled period of the c axis. This average structure contains so many vacancy sites in relation to the restriction of the chemical composition that the sites should have fractional occupancy parameters. The fractional distribution of vacancy and atom causes other subsidiary reflections in reciprocal space, and at least some of the other of the subsidiary reflections must reflect its superstructure. In fact, the present model describes all of the observed intensity distribution in reciprocal space.

Cameron (1977) has made a systematic survey of mullite of various compositions, and given a detailed description of subsidiary reflections in the $h0l$ reciprocal-lattice sections. The superstructure model in the present study, which has been derived to describe a crystal with the composition $x = 0{\cdot}186$, can easily be modified to explain the crystals within the compositional range $x = 0{\cdot}125$ to $x = 0{\cdot}2$ by varying the domain sizes and the stacking sequences. Cameron (1977) observed that the aluminium-rich specimens with $x > 0{\cdot}2$ have more complex diffraction patterns in $h0l$ sections. The structure of these specimens can be described by minor corrections of the present model.

Conclusive remark

In the present investigation, structural models of finite size were constructed. The calculated intensities which resulted from these models were then compared to the observed intensities. The experimental limitation that only the time and space average of the atomic behavior is observable by the diffraction method inevitably results in the statistical nature of the description. Therefore, the distribution of atoms or vacancies cannot be represented without the concept of probability. However, the information about the most realistic behavior is lost when the distribution of atoms or vacancies is represented by means of a fractional occupancy factor. In the present work, the statistical nature was restricted to the construction of models, and no occupancy factors were used. To date, this is the only possible means by which all coherent elastic diffraction in reciprocal space by the disordered superstructure of crystalline substances can be described.

The authors wish to express their gratitude to Professors R. Sadanaga and Y. Takéuchi at the University of Tokyo for their suggestion of this problem. They are also indebted to Mr Jack C. Ainsworth and Dr Waltraud M. Kriven at the University of California for improvements in the manuscript.

References

AGRELL, S. O. & SMITH, J. V. (1960). *J. Am. Ceram. Soc.* **43**, 69–76.

BURNHAM, C. W. (1964). *Carnegie Inst. Washington Yearb.* **62**, 158–165.

CAMERON, W. E. (1977). *Am. Mineral.* **62**, 747–755.

CROMER, D. J. & MANN, J. B. (1968). *Acta Cryst.* A**24**, 321–324.

DORNBERGER-SCHIFF, K. (1956). *Acta Cryst.* **9**, 593–601.

DUROVIC, S. (1962). *Kristallografiya*, **7**, 339–349.

GUSE, W. & SAALFELD, H. (1976). *Z. Kristallogr.* **143**, 177–187.

NAKAJIMA, Y., MORIMOTO, N. & WATANABE, E. (1975). *Proc. Jpn Acad.* **51**, 173–178.

SADANAGA, R., TOKONAMI, M. & TAKÉUCHI, Y. (1962). *Acta Cryst.* **15**, 65–68.

TAYLOR, W. H. (1928). *Z. Kristallogr.* **68**, 503–521.

TOKONAMI, M. (1965). *Acta Cryst.* **19**, 486.

WARREN, B. E. (1933). *J. Am. Ceram. Soc.* **16**, 412–421.